

Improvements in reverse characteristics of diamond Schottky diodes by neutron irradiation

Yang-Fan Li(李洋帆), Wu-Ying Ma(马武英), Ruo-Zheng Wang(王若铮), Hong-Xia Guo(郭红霞), Lin-Yue Liu(刘林月), Ze-long Niu(牛泽隆), Ru-Xue Bai(白如雪), Ji-Fang Li(李济芳), Qi Li(李奇), Hong-Xing Wang(王宏兴), and Xiao-Ping Ou-Yang(欧阳晓平)

Citation: Chin. Phys. B, 2026, 35 (**8**): 088104. DOI: 10.1088/1674-1056/ae0b37
http://cpb.iphy.ac.cn; http://iopscience.iop.org/cpb

What follows is a list of articles you may be interested in

Influence mechanism of temperature fluctuation on the growth of adjunct diamond under HPHT conditions

Yadong Li(李亚东), Minghui Jin(金明辉), Lang Xie(谢浪), Wenjing Huang(黄文静), Qing Zhang(张庆), Liangchao Chen(陈良超), Chao Fang(房超), Rui Wang(王睿), and Chunlei Du(杜春雷)

Chin. Phys. B, 2026, 35 (**6**): 068101. DOI: 10.1088/1674-1056/ae5172

Regulation mechanism of Si vacancies in unintentional silicon-doped diamond by gas flow in MPCVD

Kai Yang(杨凯), Liangxue Gu(顾梁雪), Gengyou Zhao(赵耕右), Kun Tang(汤琨), Bo Feng(冯博), Jiandong Ye(叶建东), Rong Zhang(张荣), Shunming Zhu(朱顺明), and Shulin Gu(顾书林)

Chin. Phys. B, 2025, 34 (**11**): 118102. DOI: 10.1088/1674-1056/ae07aa

Synthesis of two-dimensional diamond by phase transition from graphene at atmospheric pressure

Songyang Li(李松洋), Zhiguang Zhu(朱志光), Youzhi Zhang(张有志), Chengke Chen(陈成克), and Xiaojun Hu(胡晓君)

Chin. Phys. B, 2025, 34 (**5**): 058101. DOI: 10.1088/1674-1056/adb688

Synthesis and nitrogen content regulation of diamond in a high-pressure hydrogen-rich environment

Guofeng Huang(黄国锋), Liangchao Chen(陈良超), and Chao Fang(房超)

Chin. Phys. B, 2024, 33 (**6**): 068102. DOI: 10.1088/1674-1056/ad2a6d

High performance trench diamond junction barrier Schottky diode with a sidewall-enhanced structure

Ying Zhu(朱盈), Wang Lin(林旺), Dong-Shuai Li(李东帅), Liu-An Li(李柳暗), Xian-Yi Lv(吕宪义), Qi-Liang Wang(王启亮), and Guang-Tian Zou(邹广田)

Chin. Phys. B, 2023, 32 (**8**): 088101. DOI: 10.1088/1674-1056/acc2ae

---

Improvements in reverse characteristics of diamond Schottky diodes by neutron irradiation

Yang-Fan Li(李洋帆)[1,2], Wu-Ying Ma(马武英)[1,3], Ruo-Zheng Wang(王若铮)[3], Hong-Xia Guo(郭红霞)[1], Lin-Yue Liu(刘林月)[1], Ze-long Niu(牛泽隆)[3], Ru-Xue Bai(白如雪)[2], Ji-Fang Li(李济芳)[2], Qi Li(李奇)[3], Hong-Xing Wang(王宏兴)[3,†], and Xiao-Ping Ou-Yang(欧阳晓平)[1,‡]

[1] *Northwest Institute of Nuclear Technology, Xi'an* 710024, *China*

[2] *The School of Materials Science and Engineering, Xiangtan University, Xiangtan* 411105, *China*

[3] *Key Laboratory of Physical Electronics and Devices, School of Electronic Science and Engineering, Xi'an Jiaotong University, Xi'an* 710049, *China*

(Received 10 July 2025; revised manuscript received 2 September 2025; accepted manuscript online 25 September 2025)

Diamond is emerging as a promising material for space applications due to its unique properties and potential high performance in extreme environments. In this work, we systematically study the impact of 1 MeV equivalent neutron irradiation on diamond Schottky barrier diodes (SBDs). According to current–voltage (I–V) measurements, the Schottky barrier height (Φ_B) of the diamond SBD was increased from 1.23 eV to 1.32 eV, the ideality factor (n) was reduced from 1.88 to 1.66, and the reverse breakdown voltage increased by 100 V after neutron irradiation. Furthermore, the carrier concentration across the diamond drift layer was observed to decrease from 5.91×10^{15} cm^{-3} to 5.15×10^{15} cm^{-3} based on the capacitance–voltage (C–V) measurement. Moreover, the low-frequency noise analysis also indicated a decrease. Considering the changes in device performance, the metal/semiconductor interface traps were slightly reduced, and the Schottky barrier was significantly improved.

Keywords: diamond, Schottky barrier diode, neutron

PACS: 81.05.ug, 78.40.Fy, 61.80.Hg

DOI: 10.1088/1674-1056/ae0b37 **CSTR:** 32038.14.CPB.ae0b37

1. Introduction

Compared with other wide-gap semiconductors, diamond is a desirable material for high-power devices due to its superior physical properties,[1–7] including an ultra-wide bandgap of 5.5 eV, a higher breakdown electric field of 10 MV/cm, and a greater thermal conductivity of 22 W·cm^{-1}·K^{-1}. Meanwhile, the advancement of low-defect-density technologies and diamond doping technologies has spurred the development of diamond-based devices.[8–12] Traoré *et al.*[13] prepared a Zr/Pt/Au diamond Schottky diode that achieved a breakdown field larger than 7.7 MV/cm and a power figure of merit above 244 MW/cm^2, with good thermal stability. Additionally, the device maintained rectification characteristics at 773 K. Shao *et al.*[14] also prepared a Zr/diamond pseudo-vertical Schottky barrier diode that still displayed rectifying behavior over a wide temperature range of 298–448 K. Notably, the high performance and thermally stable rectifying characteristics make diamond Schottky barrier diodes (SBDs) strong candidates for high-temperature and rectification applications.

In theory, diamond-based semiconductor devices have stronger radiation resistance and are expected to find applications in the aerospace sector. Thus, studying the effects of space radiation on diamond-based devices is vital to accelerate their application in the aerospace industry, since radiation particles in space environments can seriously impair their reliability. Since research on the radiation effects of diamond-based devices remains limited, the theoretical potential of their radiation resistance has yet to be demonstrated.

Umezawa *et al.*[15] investigated the effects of x-ray irradiation on diamond metal–semiconductor field-effect transistors (MESFETs) and diamond Schottky barrier diodes. After 10 MGy x-ray irradiation, the forward current characteristics of diamond SBDs did not significantly deteriorate, while the leakage current density of diamond SBDs increased by at least two orders of magnitude. Therefore, Umezawa concluded that conduction through point defects in Al_2O_3 created by x-ray irradiation and adsorbates on the Al_2O_3 passivation surface from the atmosphere during x-ray irradiation could contribute to the increase in reverse current. Uncharged neutrons are the most invasive radiation particles and the primary source of displacement damage in semiconductor power devices.[9] Therefore, previous reports on diamond SBDs have mainly focused on device fabrication, whereas studies on radiation-induced damage in diamond SBDs remain limited.

In this work, we investigated the effects of neutron radiation on the electrical performance of diamond SBDs through

†Corresponding author. E-mail: hxwangcn@mail.xjtu.edu.cn

‡Corresponding author. E-mail: oyxp2003@yahoo.com.cn

© 2026 Chinese Physical Society and IOP Publishing Ltd. All rights, including for text and data mining, AI training, and similar technologies, are reserved.

experiments. By measuring *I*–*V*, *C*–*V*, and low-frequency noise (LFN), we systematically analyzed the mechanisms underlying its influence.

2. Experimental details

The diamond SBD devices used in this study are schematically shown in Fig. 1. The doping concentration of the 300 μm commercially available single-crystalline IIb-type (100) high-temperature high-pressure p^+ diamond substrate is 5×10^{19} cm^{-3}. A 3 μm unintentionally doped p^- drift layer was grown on the p^+ diamond substrate by the microwave plasma chemical vapor deposition (MPCVD) method. Additionally, the doping concentration of the p^- drift layer is around 1×10^{16} cm^{-3}. The bottom contact was achieved by depositing Ti/Pt/Au metal on the back surface of the substrate using electron-beam evaporation, followed by rapid thermal annealing. Furthermore, Zr/Au metal was fabricated as a Schottky contact on the p^- drift layer using photolithography and the lift-off technique. Notably, the radius of the Schottky electrode is 50 μm, and the thicknesses of Zr/Au are approximately 50 nm/100 nm.

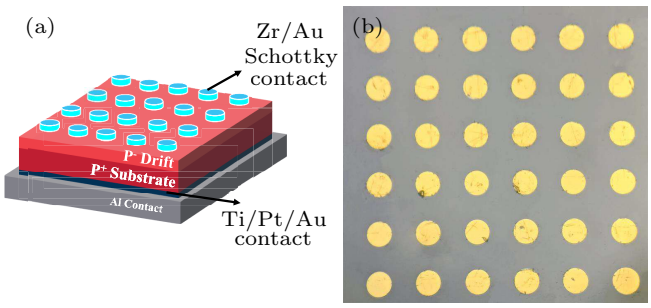


Fig. 1. (a) Cross-sectional structure and (b) top-view micrograph of fabricated diamond SBDs.

The neutron irradiation experiment was conducted in the Xi'an Pulse Reactor (XPR). The radiation field is a mixed field of neutrons and gamma rays. During the experiment, the diamond SBD devices were irradiated with a 1 MeV equivalent neutron fluence of 2×10^{11} n/cm^2 and 1×10^{12} n/cm^2. Simultaneously, the devices remained at room temperature without applying a bias voltage. The electrical characteristics were measured using a Keysight B1500A parametric analyzer, a Keysight B1505A parametric analyzer, and a low-frequency noise analyzer.

To understand the changes in the electrical characteristics of the diamond SBD devices before and after neutron irradiation, the forward *I*–*V* curves (linear coordinates) and the reverse *I*–*V* curves (semi-logarithmic coordinates) were measured as shown in Figs. 2(a) and 2(b). Notably, the performance of all devices was consistent. The current density of the device at $V = 20$ V decreased from 437 A/cm^2 to 405 A/cm^2 (a 7% reduction) after neutron irradiation with a fluence of 2×10^{11} n/cm^2. The current density of the device at $V = 20$ V decreased from 437 A/cm^2 to 370 A/cm^2 (a 15% reduction) after neutron irradiation with a fluence of 1×10^{12} n/cm^2 (Fig. 2(a)). Moreover, the turn-on voltage increased from 1.88 V to 1.95 V and 2.01 V before and after irradiation, respectively, and the $R_{\mathrm{on,sp}}$ increased from 1.18 mΩ·cm^2 to 1.38 mΩ·cm^2 and 1.55 mΩ·cm^2 after irradiation. These results indicate that the device performance was affected by neutron irradiation. From the forward and reverse *I*–*V* curves, the forward current characteristics did not significantly deteriorate, while the reverse current density of the device decreased by one order of magnitude after neutron irradiation.

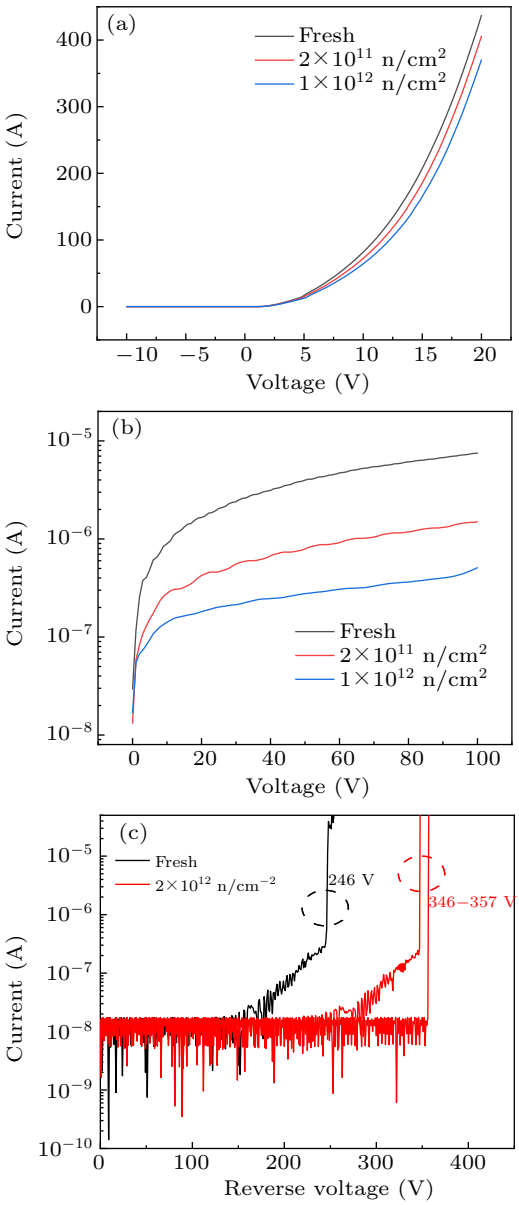


Fig. 2. (a) Forward and (b) reverse *I*–*V* characteristic curves of diamond SBDs before and after irradiation, and (c) reverse *I*–*V* characteristics of the devices. The (a) is a linear-coordinate *I*–*V* plot, while (b) and (c) are semi-logarithmic-coordinate *I*–*V* plots.

The thermionic emission (TE) model is the most widely used model to describe the current characteristics of diamond

SBDs. The forward current density (J_F) across a Schottky barrier under a forward bias voltage is expressed as[16–18]

$$J_F = J_S \exp\left(\frac{q(V - R_S J_F)}{nkT}\right), \quad (1)$$

$$J_S = A^* T^2 \exp\left(\frac{-q\Phi_B}{kT}\right), \quad (2)$$

where J_S is the saturation current density, V is the bias voltage, q is the electron charge, R_S is the series resistance, n is the ideality factor, k is the Boltzmann constant, T is the thermodynamic temperature (300 K at room temperature), A^* is the Richardson constant (96 A·cm^{-2}·K^{-2} with the effective mass of holes $m^* = 0.8m_0$),[19] and Φ_B is the Schottky barrier height at zero bias. The Schottky barrier height can be determined by extrapolating J_S using Eq. (2). Taking the logarithm of both sides of Eq. (1), $\ln J_F$ is linearly related to V. Furthermore, the slope of the linear portion of the $\ln J_F$–V plot may be used to determine the ideality factor using the relation[18]

$$n = \frac{q}{kT}\frac{\partial V}{\partial(\ln I)}. \quad (3)$$

In addition, the slope extracted from the J–V curve yielded the ideality factor $n = q/(kT)$, where s is the slope of the linear fitting from the J–V data. The Schottky barrier height (SBH) Φ_B was estimated using the obtained intercept. The values of Φ_B and n of diamond SBDs changed from 1.23 eV and 1.88 before irradiation to 1.25 eV and 1.81, and 1.32 eV and 1.66 after irradiation. It is seen that Φ_B was significantly improved, and n was slightly improved. The increase in Φ_B after irradiation correlates with reduced interface states, and the decrease in n indicates improved carrier transport due to defect passivation, consistent with radiation-hardened diamond SBDs reported in the literature.[20]

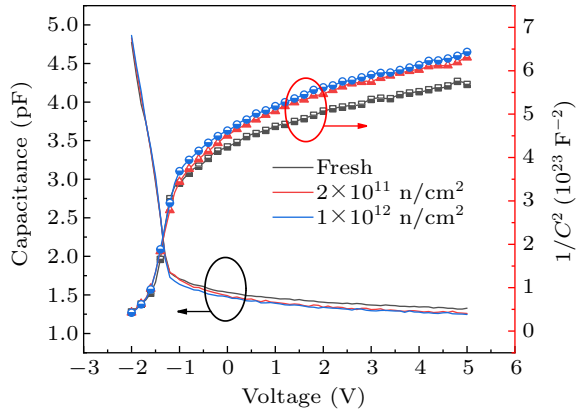


Fig. 3. The C–V and C^{-2}–V characteristics of diamond SBDs before and after irradiation at 100 kHz.

To explore the trap states generated by neutron irradiation in diamond materials, the C–V characteristics were measured using a Keysight B1500A parametric analyzer. A frequency of 100 kHz was selected to isolate the depletion capacitance from interface trap effects, enabling defect density extraction. From the C–V and C^{-2}–V curves in Fig. 3, it is noted that the capacitance decreased slightly.

The C–V relationship of SBDs is expressed as[19]

$$\frac{1}{C^2} = \frac{2}{q\varepsilon_S\varepsilon_0 N_A A^2}\left(V_{bi} - V - \frac{kT}{q}\right), \quad (4)$$

where ε_S is the permittivity of the semiconductor (5.7 for diamond), ε_0 is the permittivity of vacuum (8.85×10^{-12} F·m^{-1}), N_A is the carrier concentration in the drift layer, A is the area of the Schottky electrode, and V_{bi} is the built-in voltage.

From the slope of the fitted line of the C^{-2}–V plots at 100 kHz, the value of N_A changed from 5.91×10^{15} cm^{-3} before irradiation to 5.63×10^{15} cm^{-3} and 5.15×10^{15} cm^{-3} after irradiation.

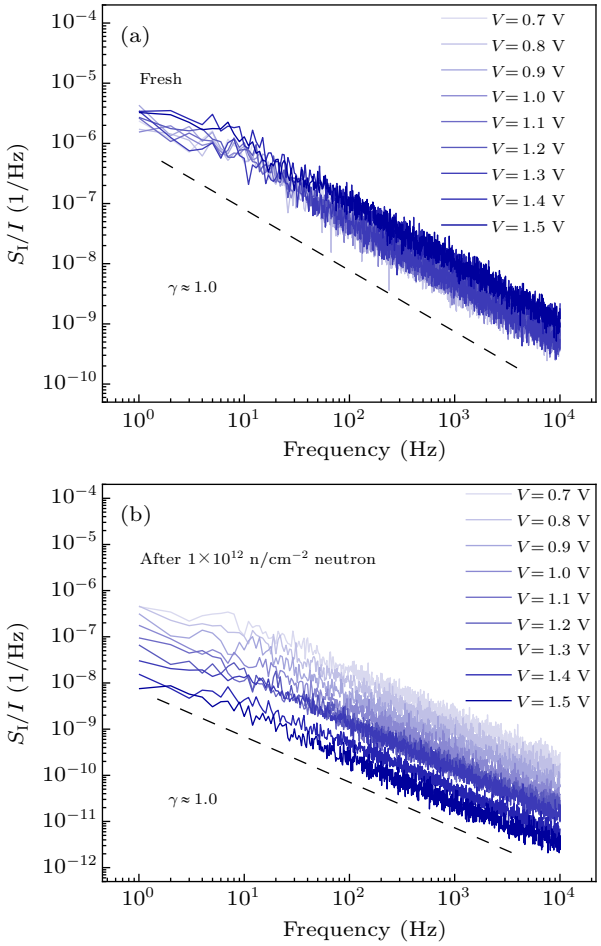


Fig. 4. Low-frequency noise spectra of voltage fluctuations in diamond SBDs before (a) and after (b) irradiation.

In the SBD, carrier transport across the metal/semiconductor interface is significantly affected by the trapping–detrapping of carriers by interface traps or barrier inhomogeneities at the metal/semiconductor interface.[21] Therefore, a low-frequency noise analyzer was used to measure the noise power spectral density of the current fluctuations of SBD devices before and after neutron irradiation at 300 K in

the voltage range of 0.7–1.5 V to study the influence of neutron irradiation on the SBD metal/semiconductor interface. The normalized results are shown in Fig. 4. Furthermore, it is noted that at frequencies of 1–10 kHz, the low-frequency noise spectra of voltage fluctuations of diamond diodes following irradiation are found to be one to three orders of magnitude lower than those of diamond diodes before irradiation over the whole voltage range.

The noise power spectral density of voltage fluctuations (S_V) is expressed as[22]

$$S_V = \frac{A\tau}{1+(2\pi f\tau)^2} + \frac{B}{f^\gamma}, \tag{5}$$

where $A\tau$ and B are the amplitudes of Lorentzian and $1/f$ noise, respectively, τ is the trapping–detrapping time during which a carrier interacts with a trap, and this process causes the GR noise. f represents the measured frequency, and γ is the frequency exponent.

The noise power spectral density of current fluctuations (S_I) is obtained from S_V using[22,23]

$$S_I = \frac{S_V}{\left(\dfrac{dV}{dI} - R_S\right)^2} = \frac{S_V}{\left[\dfrac{nkT}{q(I+I_S)}\right]^2}, \tag{6}$$

where the symbols have their usual meanings.

According to the number fluctuation model, the Lorentzian and $1/f$ noises are included in Eq. (5). When a single trap dominates the transport, the low-frequency noise behavior is Lorentzian noise; when numerous traps participate in the conduction process, Lorentzian noises are superimposed, resulting in $1/f$ noise behavior. In logarithmic coordinates, the noise power spectral density of the current, S_I, exhibits a $1/f^\gamma$ dependence with γ close to 1 for SBDs before and after irradiation in Fig. 4. Metal/semiconductor interface traps dominate carrier transport at lower bias, whereas barrier inhomogeneities govern carrier transport at higher bias.[22,24] The barrier height and interface states can affect the random capture and emission of carriers and thus influence the noise level. It is commonly known that electronic transport across metal/semiconductor interfaces is significantly influenced by interface states inside the forbidden gap, and reduced interface states result in a decreased level of $1/f$ noise.[25] Furthermore, the $1/f$ noise level strongly correlates with the strength of barrier inhomogeneities, and stronger barrier inhomogeneities result in higher $1/f$ noise levels.

The barrier inhomogeneity model, which considers both the density of interface states and the level of barrier inhomogeneities, provides a reasonable interpretation of the diamond SBD. A higher $1/f$ noise level indicates higher metal/semiconductor interface states and increased barrier inhomogeneities. Comparing Figs. 4(a) and 4(b), it is found that the $1/f$ noise was insignificantly changed at low bias and reduced at high bias after neutron irradiation. This indicates that the metal/semiconductor interface states were not significantly reduced, whereas the barrier inhomogeneities were improved. Moreover, the improved barrier inhomogeneities directly lead to a decrease in the forward and reverse current densities of the device, which corresponds to the data in Fig. 2.

Reverse breakdown voltage is a vital diode characteristic that directly impacts the application of devices in contemporary industrial and consumer power electronics. Thus, to explore the influence of neutron radiation on the device breakdown voltage (V_{BR}), the reverse current–voltage characteristics of the diamond SBDs were measured using a Keysight B1505A parametric analyzer before and after neutron irradiation. The voltage corresponding to the moment of current surge is defined as the breakdown voltage. The typical results of the reverse I–V characteristics of the diamond SBDs before and after irradiation are shown in Fig. 2(c). It can be seen that the maximum breakdown voltage of the fresh SBDs reaches 246 V. In comparison, the maximum breakdown voltage is 357 V for the neutron-irradiated devices. It is also observed that neutron irradiation increases the device breakdown voltage by more than 100 V. Notably, this confirms that the Schottky barrier of the device has been significantly improved.

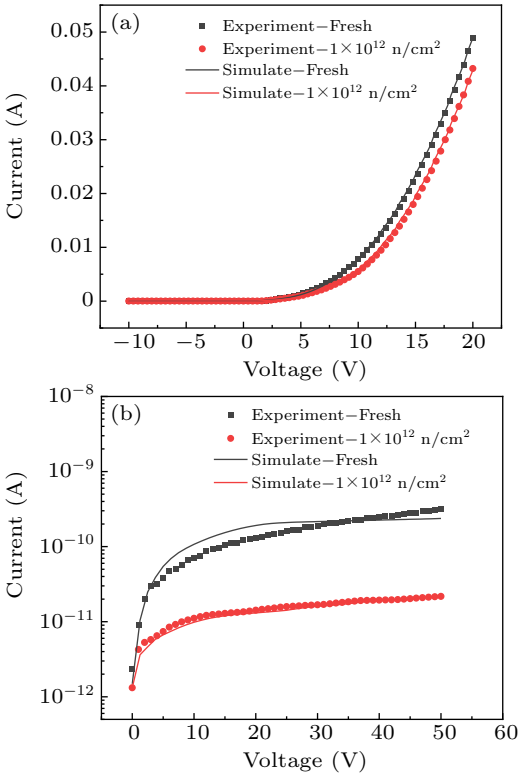


Fig. 5. (a) Forward and (b) reverse I–V characteristic curves of diamond SBDs before and after irradiation.

A two-dimensional (2D) numerical device simulation was performed using TCAD software. Based on the C–V data, only the carrier concentration within the epitaxial layer was

changed during the simulation. The forward and reverse *I*–*V* characteristic curves of diamond SBDs obtained from the simulation are shown in Fig. 5. The simulation results are almost consistent with the experimental data by changing the carrier concentration. Notably, this indicates that the improvement in the electrical performance of diamond devices is also attributed to the generation of bulk traps after neutron irradiation.

3. Conclusion and perspectives

In conclusion, the effect of neutron irradiation on the electrical performance of diamond devices has been studied experimentally in this work. It was discovered that the electrical properties of the devices were slightly degraded after neutron irradiation, while the breakdown performance was significantly improved. This can be explained by the improved barrier inhomogeneities and decreased interface state traps following neutron irradiation. Additionally, *C*–*V* measurements and corresponding calculations show that the carrier concentration within the drift layer slightly decreased after neutron irradiation. Meanwhile, the $1/f$ noise results demonstrate that the Schottky barrier was significantly improved after neutron irradiation. Thus, the reverse characteristics of diamond SBDs following neutron irradiation were improved, suggesting that neutron irradiation may be applied as a manufacturing step to enhance device performance. The results also show that diamond SBDs exhibit robust neutron resistance. The results of this work can offer valuable insights for improving the reliability of diamond SBDs.

References

[1] Volpe P N, Muret P, Pernot J, Omnès F, Teraj T, Koide Y, Jomard F, Planson D, Brosselard P, Dheilly N, Vergne B and Schamholz S 2010 *Appl. Phys. Lett.* **97** 223501

[2] Umezawa H, Nagase M, Kato Y and Shikata S I 2012 *Diamond Relat. Mater.* **24** 201

[3] Umezawa H, Nagase M, Kato Y and Shikata S I 2013 *Diamond Relat. Mater.* **40** 56

[4] Umezawa H, Shikata S I and Funaki T 2014 *Jpn. J. Appl. Phys.* **53** 05FP06

[5] Seok O and Ha M W 2021 *Jpn. J. Appl. Phys.* **60** SCCE08

[6] Lo Q, Wang J, Chen G Q, He S, Zhang Q W, Zhang S M, Wang R Z, Fan S W and Wang R Z 2023 *Diamond Relat. Mater.* **134** 109799

[7] Mu L X, Zhao S M, Wang P, Yuan X L, Liu J L, Zhu Z F, Chen L X, Wei J J, Ouyang X P and Li C M 2024 *Chin. Phys. B* **33** 026801

[8] Ohmagari S, Teraji T and Koide Y 2011 *Jpn. J. Appl. Phys.* **110** 056105

[9] Umezawa H, Kato Y, Watanabe H, Omer A, Yamaguchi H and Shikata S I 2011 *Diamond Relat. Mater.* **20** 523

[10] Kato Y, Umezawa H, Shikata S I and Touge M 2013 *Appl. Phys. Express* **6** 025506

[11] Liu D Y, Tang K, Zhu S M, Zhang R, Zheng Y D and Gu S L 2023 *Chin. Phys. B* **32** 118102

[12] Zhu Y, Lin W, Li D S, Li A L, Lv X Y, Wang Q L and Zou G T 2023 *Chin. Phys. B* **32** 088101

[13] Traoré A, Muret P, Fiori A, Eon D, Gheeraert E and Pernot J 2014 *Appl. Phys. Lett.* **104** 052105

[14] Shao G Q, Wang J, Wang Y, Wang W and Wang H X 2022 *Sens. Actuators, A* **347** 113906

[15] Umezawa H, Ohmagari S, Mokuno Y and Kaneko J H 2017 *29th International Symposium on Power Semiconductor Devices and IC's (ISPSD)* pp. 379

[16] Sze S M, Li Y and Ng K K 1981 *Physics of Semiconductor Devices* (Wiley)

[17] Baliga B 2010 *Fundamentals of Power Semiconductor Devices* (Springer)

[18] Malakoutian M, Benipal M, Koeck F A, Nemanich R J and Chowdhury S 2020 *IEEE J. Electron Devices Soc.* **8** 614

[19] Wand J, Zhao D, Shao G Q, Liu Z C, Chang X H, Chen G Q, Wang W, Yi W Y, Wang K Y and Wang H Y 2021 *IEEE Trans. Electron Devices* **68** 1176

[20] Fiori A, Teraji T and Koide Y 2014 *Appl. Phys. Lett.* **105** 133515

[21] Kumar A, Latzel M, Christiansen S, Kumar V and Singh R 2015 *Appl. Phys. Lett.* **107** 093502

[22] Kumar A, Kumar V and Singh R 2016 *J. Phys. D: Appl. Phys.* **49** 47LT01

[23] Kumar A, Asokan K, Kumar V and Singh R 2012 *J. Appl. Phys.* **112** 024507

[24] Singh R and Kanjilal D 2002 *J. Appl. Phys.* **91** 411

[25] Maes H E, Usmani S H and Groeseneken G 1985 *J. Appl. Phys.* **57** 4811